Talanta 120 (2014) 173–180

Contents lists available at ScienceDirect

Talanta

journal homepage: www.elsevier.com/locate/talanta

Development of an electrospray-^{63}Ni-differential ion mobility spectrometer for the analysis of aqueous samples

Andriy Kuklya [a,*], Florian Uteschil [a], Klaus Kerpen [a], Robert Marks [a], Ursula Telgheder [a,b]

[a] Department of Instrumental Analytical Chemistry, University of Duisburg-Essen (UDE), Universitätsstraße 5, 45141 Essen, Germany
[b] IWW Water Centre, Moritzstr. 26, 45476 Mülheim a.d. Ruhr, Germany

ARTICLE INFO

Article history:
Received 17 August 2013
Received in revised form
14 October 2013
Accepted 20 October 2013
Available online 11 December 2013

Keywords:
Differential ion mobility spectrometry (DMS)
High field asymmetric waveform ion mobility spectrometry (FAIMS)
Electrospray (ES)
Aqueous samples
Water monitoring
Online monitoring

ABSTRACT

The feasibility of an electrospray coupled with a ^{63}Ni-differential ion mobility spectrometer (DMS) for the analysis of water samples was proven on examples of 2-hexanone, fluoroacetamide, L-nicotine and 1-phenyl-2-thiourea water solutions. The model substances were selected in order to cover the vapor pressure range of 0.3–1467 Pa. To reduce the inline humidity, which demonstrates a strong influence on the analyte compensation voltage, two units with a desolvation region lengths of 15.5 and 7 mm were examined. The counter gas (heated to 100 °C nitrogen) with flow rates of 100 mL min^{-1} and 30 mL min^{-1} for short and long desolvation units, respectively, was essential for the efficient reduction of humidity. The reduction of water content in the carrier gas to 2.2–2.4 g m^{-3} and to 1.8–2.0 g m^{-3} for the short and long desolvation unit, respectively, was achieved at an electrospray flow rate of 1000 nL min^{-1}. With this adjusted experimental setup, the detection of model substances in the water solutions, in the range of 0.1–50 mg L^{-1}, was performed. No correlation between the vapor pressure and signal area was observed. The high stability of the inline humidity, and the correspondingly stable carrier gas flow rate, were found to be essential for an acceptable reproducibility.

© 2013 Elsevier B.V. All rights reserved.

1. Introduction

The quality of drinking water is an important issue nowadays. Due to the potentially rapid spread of water contaminants within the public distribution network, the continuous improvement of an early warning systems, and the development of new online water monitoring methods is essential. However, most of the existing methods are laboratory-based and therefore require sampling. In many cases the derivatization or extraction steps are required. Therefore, interest in simple, inexpensive, and fast techniques for on-site monitoring has grown in recent years.

In this paper, the development of a new method of measuring aqueous samples, by means of planar differential ion mobility spectrometry (DMS), also known as planar high field asymmetric waveform ion mobility spectrometry (FAIMS), is described. This method allows for the analysis of aqueous samples directly from the liquid phase and requires no extraction or derivatization steps. The presented method involves the nebulization of the liquid sample by the electrospray (ES), the subsequent desolvation of the analyte, and lastly, the ionization by ^{63}Ni source.

The DMS is a rapidly advancing technology that is both sensitive and fast, operates at atmospheric pressure, and provides a unique type of selectivity, which is orthogonal to most of other separation techniques.

The working principle of DMS is based on the nonlinear dependence of the ion mobility coefficient ($K_{(E)}$) on the applied electric field. In contrast to the conventional Time of Flight Ion Mobility Spectrometry (ToF-IMS), in which the separation of ions is based on specific coefficients of ion mobility in a uniform electric field, DMS separates ions based on a nonlinear dependence of the mobility coefficient on the electric field strength.

The DMS separation ability is based on the utilization of a high frequency periodical wave function containing both the high and the low field components. Due to the nonlinear dependence of the ion mobility coefficient on the electric field, the net displacement of the ions during each oscillation is proportional to the difference of the ion mobility coefficients at the high and low electric fields.

The dependence of the ion mobility coefficient on the electric field can be explained by the reversible cluster formation model, which describes field dependent cluster formations that lead to variation of the average ion cluster cross section [1]. The functional principles of the DMS are described elsewhere [2,3].

In the last decade, a huge number of publications have described the measurements of gaseous samples using DMS/FAIMS, and liquid samples using DMS/FAIMS-MS coupling, but there are only a few examples of the successful application of stand-alone DMS or FAIMS for liquid sample measurements [4–7]. However, many of the analytes have a low Henry constant, and as

* Correspondence to: Department of Instrumental Analytical Chemistry, University of Duisburg-Essen (UDE), Universitätsstraße 5, 45141 Essen, Germany. Tel.: +49 201 183 6786; fax: +49 201 183 6773.
E-mail address: andriy.kuklya@uni-due.de (A. Kuklya).

0039-9140/$ - see front matter © 2013 Elsevier B.V. All rights reserved.
http://dx.doi.org/10.1016/j.talanta.2013.10.056

a result, cannot be effectively detected by the headspace analysis. Therefore, the development of analytical methods for the detection of nonpolar compounds of limited volatility, directly from the water phase, is essential.

ESI, atmospheric pressure photo ionization (APPI), and atmospheric pressure chemical ionization (APCI) are the most frequently used ionization techniques, which enable the analysis of the analyte from the liquid samples in the gas phase.

ESI was introduced in 1985 by Fenn and coworkers as a soft ionization method for the liquid chromatography-MS interface [8]. In this method, the solution is sprayed by means of a high voltage followed by a rapid but gentle desolvation. This method works perfectly for the ionization of polar compounds, which can be protonated or deprotonated well. However, for the ionization of nonpolar compounds the application of electrospray ionization is very limited and frequently involves a derivatization of the nonpolar analyte [9].

APPI is a relatively new method applied in 2000 for liquid chromatography-MS coupling [10,11]. With this method it was expected to extend the range of ionizable compounds of low polarity. However, except for some aromatic polycyclic compounds [12], the range of compounds that can be efficiently ionized by APPI is similar to that of APCI [10,13].

The first APCI source for mass spectrometry was developed in 1973 by Horning et al. [14]. In the APCI, the analyte solution is usually introduced into a heated pneumatic nebulizer and sprayed over a corona discharge needle or a ß-ionization source (e.g. ^{63}Ni). The MS spectra obtained with corona and with ^{63}Ni ionization are usually identical, so the ionization mechanism is assumed to be the same [15].

The ionization conditions in APCI are considered to be somewhat "harder" than those in ESI. Therefore, it is assumed to be more suitable for less polar analytes, but acid-base reactions are still the most frequently observed analyte ionization mechanisms [13].

On the other hand, the effective ionization of the nonpolar compounds by means of ion mobility based devices, equipped with ^{63}Ni or corona ionization sources similar to those that used in APCI, was proven on many occasions [16,17].

The high water concentration in a gas mixture, originating from the nebulization of the water containing analyte (A), leads to the formation of heavy analyte-water clusters with a high water content (e.g. $A(H_2O)_n^+$). These clusters have a low mobility with negligible discrimination between the different analyte-water clusters. This makes the sample analysis by means of FAIMS difficult. Thus, the water content in the gas mixture should be kept at a low value. Therefore, efficient desolvation of the analyte prior to entering of the DMS detector is required.

2. Experimental section

In this study the electrospray (ES) was utilized for the nebulization of liquid samples with nano- to microliter per minute flow rates. This method of nebulization does not require sheath gas and accelerates the produced droplets in the applied electric field. Electrospray has a number of advantages over mechanical nebulizers. The droplets, which range in size from hundreds of micrometers down to several tens of nanometers, can be controlled to some extent by the liquid flow rate and the voltage applied to the capillary. Moreover, the size of the electrospray droplets can be nearly monodisperse [18]. The ionization of the analyte, prior to entering the DMS separation chamber, is performed by a ^{63}Ni ionization source. The use of the second ionization source, embedded into the DMS, allows the use of a desolvation unit, which is arbitrarily variable in length, with only a minor reduction of the ion flow entering the DMS. Due to this modification, the design of the ES-^{63}Ni-DMS is more adjustable to experimental and constructional demands.

The mechanism of the analyte ionization by a ^{63}Ni ionization source is similar to the usual for a corona-based APCI ionization pathway [15]. In contrast to a monopolar ion source, like ESI, which is usually used for liquid sample analysis by means of DMS, ^{63}Ni ionization generates positive as well as negative ions. Direct ionization following nebulization, which takes place in the classical APCI source, was assumed to be inadequate for the current method due to the high water content in the spray, which leads to high clustering rates at atmospheric pressure, and a longer time of flight of ions to the detector, which leads to a significant drop in the signal intensities. To reduce the water content in the gas mixture, a desolvation unit was built in between the electrospray and the ionization units (see Fig. 1). In this unit, the water content is reduced by the flow of heated nitrogen in the opposite direction to the electrospray.

2.1. Electrospray unit

The conic electrospray emitters were produced out of commercially available capillaries of O.D. of 160 μm and an I.D. of 60 μm (Hamilton, USA). The reproducible cutting and etching of the emitters are important steps in order to ensure reliable results. These steps were conducted under defined conditions, and controlled microscopically. The etching was performed in accordance with the method described by Ishihama et al. [19] electrochemically in a 1:1:1H_2SO_4:H_3PO_4:H_2O solution with a 2 cm^2 Pt-counter-electrode in two steps. The first etching step was applied to a 1 cm deep immersed tip end for 2 min (9 V DC pulse, 50 Hz, duty cycle = 50%). The second etching step was applied to the tip end (less than 1 mm) of the capillary under the same conditions until no bubble formation was observed. The tip of the conic capillary was polished vertically with a turning piece of wet 2000 mesh sandpaper to avoid undesirable burs on the tip of the capillary (see Supporting information, Fig. S-1).

The homemade electrospray source was operated in a continuous injection mode. The analyte solutions were injected via a syringe pump (kdScientific, KDS Legato 210) equipped with a Hamilton gas-tight syringe of 500 μL size, connected to a stainless steel emitter, produced as described above, over the fused silica capillary (300 μm ID, 300 mm long), with flow rates of 250–2500 nL min^{-1}. The stainless steel emitter was connected to a high voltage power supply (iseg, T1DP 050 205 EPU) and the counter electrode (brass *Swagelok* 1/8 in. Tee) was connected to the ground. When the potential difference of the electrodes was within a range of 2.3–2.5 kV (positive polarity) and the electrode distance was 2 mm, the electrospray was stable for at least 2 h.

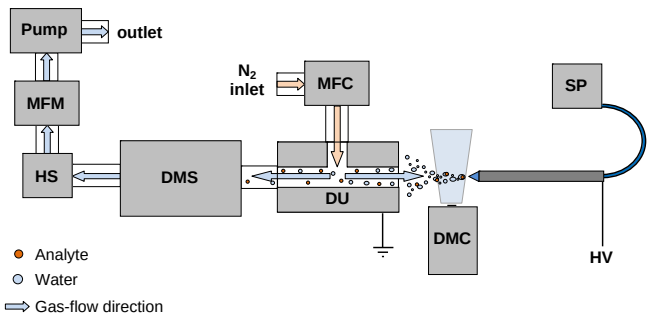

Fig. 1. The principle scheme of the experimental setup: desolvation unit (DU), differential ion mobility spectrometer (DMS), humidity sensor (HS), mass flow controller (MFC), mass flow meter (MFM), syringe pump (SP), and digital microscope camera (DMC).

Observations of the electrospray were performed with a DigMicro 2.0 (DNT, Germany) digital microscope.

2.2. Desolvation unit

Two modifications of the desolvation unit (DU) were utilized in this study (see supporting information, Fig. S-2). One was built from the original brass *Swagelok* 1/8 in. Tee (long desolvation unit). The other was a brass Swagelok 1/8 in. Tee, truncated from the electrospray side (short desolvation unit). The truncated side was mechanically modified in order to reproduce the original inner tapered joint part, for a comparable spray generation. The desolvation gas in the Tee-piece was kept at a temperature of approximately 85 °C. The nitrogen flow, which was controlled by a mass flow controller (MFC, Pneutronics, VSO-GC), was directed towards the desolvation unit. In the desolvation unit, the nitrogen flow was split into two parts. The main flow (400 mL min^{-1}) was pumped (Rotary Vane Pump, Thomson, G 045) towards the DMS (Sionex Corporation, SVAC-V, ^{63}Ni 185 MBq) carrier gas inlet, and the minor flow (30 mL min^{-1} for long desolvation unit and 100 mL min^{-1} for short desolvation unit) was directed towards the electrospray. The water content during the experiment was controlled by the HIH4000 Honeywell humidity sensor. The transfer line between the DU and DMS, built from a 15 cm long stainless steel capillary (1/8 in. O.D., 1/16 in. I.D.), was heated to 100 °C, in order to keep the analyte in the gas phase.

2.3. DMS

For each probe, four single measurements were collected, using Sionex Expert software at the fixed electric field of 30 kV cm^{-1} (1500 V), and then averaged. For the determination of peak centers and areas, the measured data were analyzed by the fityk (version 0.9.4) program [20]. The ion signals were fitted with Gaussian functions using the Levenberg–Marquardt algorithm.

DMS settings were as follows: sensor temperature=60 °C, compensating voltage range from −43 to +15 V, number of scans=200, step duration=50 ms, step settle time=3 ms, steps to blank=1, the measurements were analyzed in the positive (positive ions) and negative (negative ions) modes, otherwise noted.

2.4. Chemicals

To verify the proposed method for liquid sample analysis, solutions of four model compounds of different volatility were analyzed in a concentration range of 0.1–50 mg L^{-1}. 2-Hexanone (Sigma-Aldrich, 98%), fluoroacetamide (Acros, 98%), L-nicotine (Acros, 99+ %), and 1-phenyl-2-thiourea (Acros, 97%) were selected as model substances. The vapor pressures of the selected compounds, covering a range of 0.3–1467 Pa, are summarized in Table 1. The vapor pressures of 2-hexanone and L-nicotine are matching in most of the sources (1467 and ~5 Pa at 25 °C, respectively). With regards to the vapor pressure of fluoroacetamide and 1-phenyl-2-thiourea, the information within the literature is limited to calculated data. The vapor pressures of 132 Pa for fluoroacetamide, and of ~0.3 Pa for 1-phenyl-2-thiourea, were estimated using a fragment constant method [21,22].

Table 1
List of compounds used in the current study with the corresponding vapor pressures.

Compound	Vapor pressure at 25 °C [Pa]	Source
2-Hexanone	1467	Ref. [23]
Fluoroacetamide	~132	Ref. [22]
L-Nicotine	~5	Refs. [24,25]
1-Phenyl-2-thiourea	~0.3	Refs. [21,22]

3. Results and discussion

3.1. Electrospray mode

A strong dependence of the DMS signal's shape and intensity on the electrospray mode was observed. During the measurements with a long desolvation unit, the formation of the Taylor cone with a considerable jet (Fig. 2b) was necessary to provide stable analyte signal generation. For the spray with no Taylor cone formation (Fig. 2a), with a pulsed jet, and with multi-jet, zero to negligible signals were observed. The probable cause of this effect is the more efficient transport of the analyte within the electrospray jet, resulting in the formation of the plume in deeper regions of the desolvation unit. In the case of a multi-jet or of no jet formation, the analyte needs to diffuse over a 15.5 mm distance, which leads to a significant drop in the analyte concentration within the gas entering the DMS.

(a) No formation of Taylor cone or the Taylor cone with a pulsed jet, the potential difference is too low,
(b) formation of the stable cone-jet at proper potential difference, and
(c) formation of the multi-jet, the potential difference is too high.

Bottom, the representative peak shapes measured with cone-jet (jet) and with multi-jet.

In measurements using a short desolvation unit (distance of the desolvation pass is 7 mm) the electrospray with multi-jet formation (Fig. 2c) resulted in irreproducible signals of high area with irregular shape, or in broadening of signals. The anomaly of the peak shape was attributed to the instability of the gas phase humidity, which was observed during multi-jet formation. Using a relatively longer integration time (50 ms) results in the superposition of the analyte signals, which appear at different compensation voltages at varying humidity.

3.2. Counter gas flow rate

To investigate the influence of the counter gas flow rate, the 20 mg L^{-1} solution of fluoroacetamide in water was measured at varied counter gas flow rates, with an electrospray flow rate of 1000 nL min^{-1}.

The influence of counter gas flow rate on the fluoroacetamide signal area and carrier gas humidity, using the short and long desolvation units, is shown in Fig. 3. At fixed electrospray flow rates, the humidity observed with a long desolvation unit was lower than that observed with the short desolvation unit, which is evidence of a more efficient analyte desolvation.

When the short desolvation unit was utilized, the fluoroacetamide signal area rose, despite the likely reduction of the analyte amount entering the DMS due to the increased counter gas flow rate. In this unit, the length of the desolvation region is less than half (7 mm to 15.5 mm) that of the long desolvation unit, and diffusion of the analyte through the desolvation region plays a minor role. The increase of the signal area, however, correlates significantly with a simultaneous decrease of the carrier gas humidity, and hence, both observations can be matched. With an increase in the counter gas flow rate, it was difficult to get a stable jet formation, which is depicted by an increase in the signal area standard deviation. At flow rates higher than 100 mL min^{-1} the

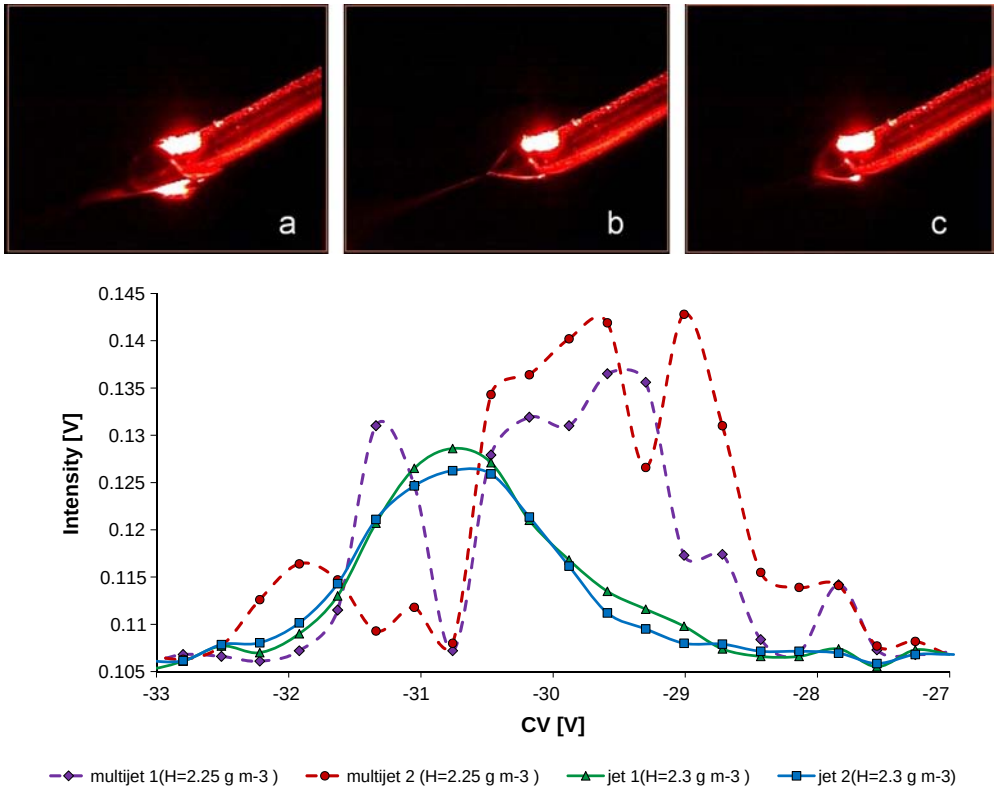

Fig. 2. Top, dependence of the electrospray mode on the applied potential difference.

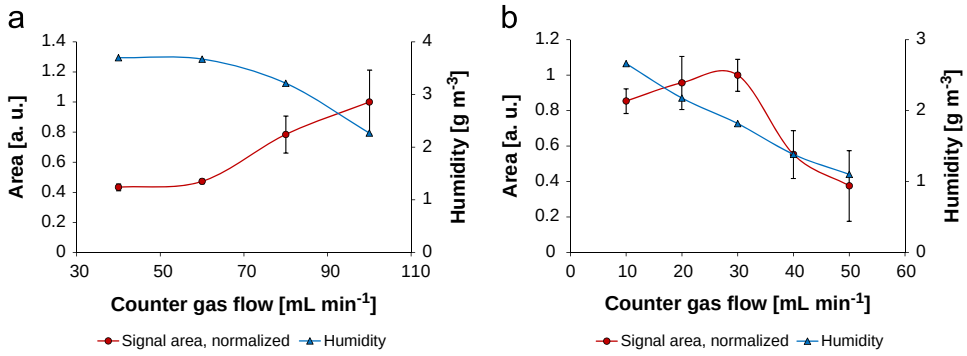

Fig. 3. Dependences of the carrier gas humidity and the signal area of a 20 mg L^{-1} fluoroacetamide solution in water on the counter gas flow rate, using the short (a) and the long (b) desolvation units.

formation of the jet was almost not realizable and therefore further increase of the counter gas flow rate was avoided.

When the long desolvation unit was utilized, the humidity dropped with an increase in the counter gas flow rate, analogous to the experiments with the short desolvation unit. The fluoroacetamide signal area demonstrates an initial increase up to the counter gas flow rate of 30 mL min^{-1}, and then continuously drops from this point. At flow rates higher than 50 mL min^{-1}, the signal was no longer detectable [signal to noise ratio (S/N) < 3]. The initial increase of the signal area can be attributed to a reduction of the carrier gas humidity, similar to that observed with the short desolvation unit. At counter gas flow rates higher than 30 mL min^{-1}, the inline humidity, which was in general lower than that observed with the short desolvation unit, reached a rather low level and no longer affected the signal area significantly. At these flow rates, diffusion of the analyte over the relatively long desolvation region, plays a dominant role.

3.3. Dependence of the compensation voltage on the humidity

The experiments performed with electrospray flow rates within the range of 250 to 3000 nL min^{-1}, demonstrate a high dependence of the compensation voltage on the concentration of water in the carrier gas. The combined data for all four compounds investigated in this study, within a humidity range of 1–5 g m^{-3}, and performed with both desolvation units, are shown in Fig. 4. To perform the measurements with a humidity of 4 g m^{-3} or higher, the counter gas flow for the short desolvation unit had to be reduced from 100 mL min^{-1} down to 40 mL min^{-1}, with an electrospray flow rate of 3000 nL min^{-1}. The analyte peaks in the measurements, with both desolvation units, appear at a comparable compensation voltage at the same humidity.

The peak position on the CV scale demonstrates a high dependence even on minor gas phase humidity variation. This dependence is especially significant in the humidity range of 1–2 g m^{-3}

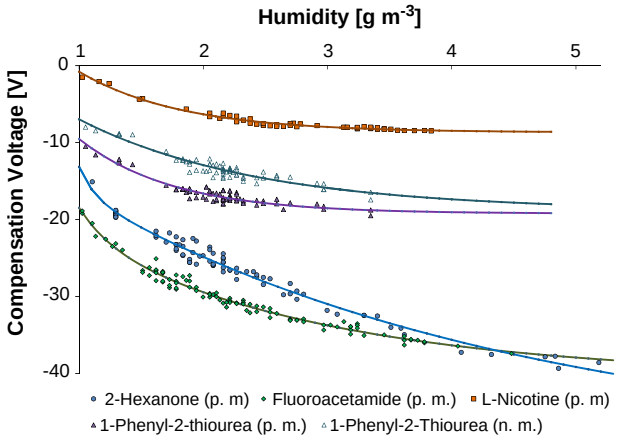

Fig. 4. Dependences of 2-hexanone, fluoroacetamide, L-nicotine, and 1-phenyl-2-thiourea compensation voltage (CV) on the carrier gas humidity at an electric field of 30 kV cm^{-1} (1500 V) in the positive mode (p.m., positive ions) and in the negative mode (n.m, negative ions).

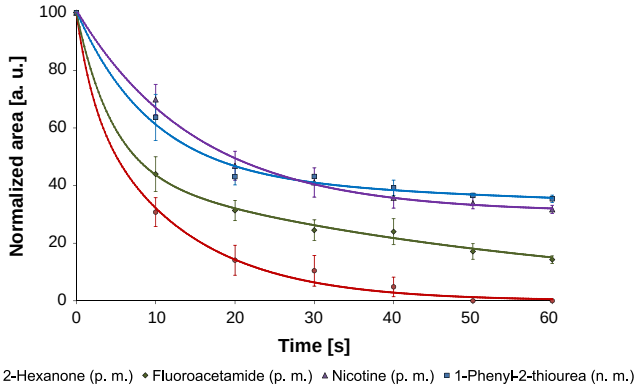

Fig. 5. Normalized residual signal areas of 2-hexanone, fluoroacetamide, and L-nicotine, in the positive mode (positive ions, p.m.) and for 1-phenyl-2-thiourea in the negative mode (negative ions, n.m.). The single measurements are fitted with an exponential function.

(see Fig. 4). Therefore, the precise humidity control during the experiment is of great importance for the achievement of reproducible experimental data.

It should be mentioned that the shift of the analyte peak compensation voltage, corresponding to an increase of the water content, improves the DMS separation capability. This enhances differentiation of the analytes, especially those whose signals have adjacent compensation voltages. The influence of moisture on the ion shift, for the DMS with the ^{63}Ni-ionization source, was demonstrated with organophosphorus compounds by Eiceman et al. [26] and later by Krylov et al. [1]. The same effect, achieved by the addition of polar modifiers to the transport gas, is reported by Schneider et al. [27].

The increase of separation ability can be explained by the reversible cluster formation model [1]. This model demonstrates that the water to analyte cluster size, and the cluster mobility, are dependent on the concentration of the clustering particles (in this case, on nitrogen, water, and analyte), cluster temperature, and complex formation energy. With an increase of electric field strength, the effective cluster temperature rises, resulting in a rapid declustering due to a high collision rate at atmospheric pressure. Hence, the average cluster size is reduced. A reduction in the average cluster size may increase ion mobility significantly. Under a low electric field, a higher water concentration in the gas phase leads to an increase in the average cluster size. An increase in the cluster cross-section, which correlates with the humidity, results in reduced cluster mobility and a corresponding increase in frequency of cluster to carrier gas collisions. As a result, the difference between mobility of the ions in the low and in the high electric fields at a higher humidity increases, leading to a higher shift of the analyte. Therefore, a higher (positive or negative) compensation voltage is required for the analyte detection.

3.4. Memory effect

DMS is known for being a very fast and sensitive method, which usually requires a pre-separation step to avoid the presence of a compounds mixture in the ionization and separation region. The presence of several compounds in DMS at the same time can lead to analyte–analyte cross clustering, charge transfer, and other undesirable processes [28]. These processes lead to alterations in individual analyte signal areas, which results in false quantifications. Therefore, the LC pre-separation step is essential for DMS based systems, which applied in the liquid sample analysis. The low volatility of the analytes can possibly influence a residence time for the compounds in the DMS system. This results in peak tailing, which indicates that better pre-separation may be required.

The 20 mg L^{-1} solutions of each compound were sprayed for 20 min through the system, to check for the memory effects of the system for the selected compounds, in the current experimental setup under extreme conditions. After 20 min, the syringe pump and the electrospray source were switched off, and the residual analyte signal was measured. For each analyte three single measurements were conducted and averaged, data are plotted in Fig. 5.

Residence time of the compounds increases in accordance with vapor pressures (see Table 1). Even for the 2-hexanone, which is a relatively volatile compound, the residual signal was observed for 30–40 s after the electrospray was switched off. For the compounds with the limited volatility, e.g. L-nicotine and 1-phenyl-2-thiourea, the area of the signal after 60 s was about 40% that of the initial level.

The dead volume of the transfer lines, between the electrospray source and the DMS, is less than 1 mL, which at carrier gas flow rate of 400 mL min^{-1} should not have had a significant influence on the obtained results. In this study, all transfer lines between the electrospray source and the DMS were heated, to keep the inline gas temperature at approximately 85–100 °C. The detector temperature was kept at only 60 °C. Under these conditions, condensation of the analyte on the DMS sensor cannot be excluded. A temperature of 60 °C was selected for sufficient resolution between the analyte and the residual ion-water cluster peaks, which was found to be reduced with the increase of temperature [29,30]. The increase of the sensor temperature to 80 and to 100 °C had a minor influence on the memory effects. Therefore, the observed effect is related to the retention effect of the transfer line. It should be mentioned, that in real samples, the appearance of such high analyte amounts are not probable. Nevertheless, to avoid the undesired retention effects, the transfer line should be heated to higher temperatures.

3.5. Concentration dependence

The aim of the current study was not to optimize the DMS parameters for the measurements of the chosen model compounds. Therefore, it is possible and even probable, that at other electric field strengths and/or DMS sensor temperatures, analyte signals of higher intensity and/or spectra with better peak separation can be obtained. The aim of the current study was to demonstrate applicability of the proposed method for the analysis of water samples. For this purpose, the dependence of the analyte signal area on the analyte concentration in water was investigated.

The signal intensity, as well as humidity, demonstrates a relatively high dependency on the position of the electrospray emitter. This is especially important for the short desolvation unit, in which the desolvation region is very short, and even a minor difference in the electrospray needle position can have a large effect. Another important issue is the precise control of the gas flow rate in the desolvation unit. This parameter is equally essential for both desolvation units. Deviation of the counter gas flow, within a range of 5–10 mL min^{-1}, can lead to significant humidity variations (see Fig. 3), and hence, to broadening of signals. This makes accurate quantification, especially at low analyte concentrations, difficult. Therefore, precise control over experimental conditions is crucial for reproducible results.

During the collection of the data presented in the current chapter, the electrospray emitter was at an approximately identical position (2 mm electrode distance) in all of the measurements. The counter gas flow was kept at rates of 100 ± 5 mL min^{-1} and 30 ± 5 mL min^{-1} for long and short desolvation units, respectively.

The DMS spectra of 2-hexanone and L-nicotine solutions, in positive mode (detection of the positive ions), within a concentration range of 0.5–50 mg L^{-1}, are shown in Fig. 6. These measurements were performed at an electric field strength of 30 kV cm^{-1} (RF=1500 V), and an ES flow rate of 1000 nL min^{-1}. The DMS spectra of fluoracetamide in positive mode, and 1-phenyl-2-thiourea solutions in both positive and negative modes (detection of the negative ions), within a concentration range of 0.1–40 mg L^{-1} and under the same experimental conditions, can be found in Supporting information. L-Nicotine was the only compound measured at an ES flow rate of 2000 nL min^{-1}. This modification was performed to increase the resolution between the analyte and residual water cluster ion signals.

The reason for the observed minor variations in the analyte peak shapes and compensation voltages, is a deviation of the relative humidity in the gas phase during these measurements. The humidity was within a range of 1.8 to 2.0 g m^{-3} and 2.2 to 2.4 g m^{-3}, with the ES flow rates of 1000 and 2000 nL min^{-1}, respectively, when the long desolvation unit (counter gas flow of 30 mL min^{-1}) was utilized. With the short desolvation unit the humidity was within a range of 2.2–2.4 g m^{-3} and 3.2–3.4 g m^{-3}, with the ES flow rates of 1000 and 2000 nL min^{-1}, respectively. The unstable water concentration during the experiment, resulted in a signal broadening that is especially significant due to longer signal integration times. However, the peak area does not depend significantly on the water concentration variation caused by the observed instability of humidity.

For all of the analytes a common for nondirect ionization mechanisms, such as APCI, nonlinear signal area to concentration relationship was observed [28].

The amount of analyte ion formed in the ionization region is dependent on the residence time of the sample in the source, as well as on the concentration of sample [A] and the reactant ion [RI].

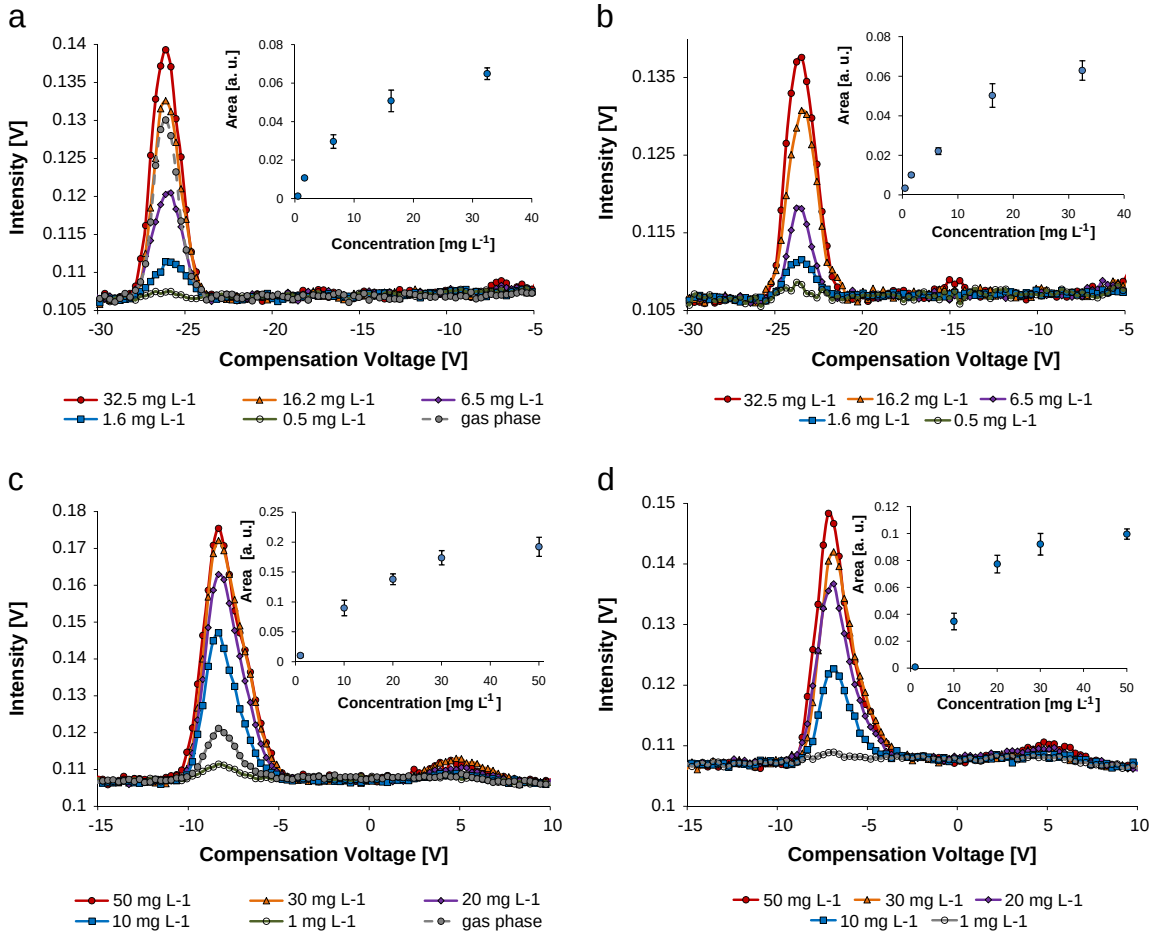

Fig. 6. DMS spectra (positive mode) of 2-hexanone solutions within a concentration range of 0.5–50 mg L^{-1} (ppm), using a short (a) and long (b) desolvation unit, and of L-nicotine solutions with short (c) and long (d) desolvation units. RF=30 kV cm^{-1} (1500 V) and DMS spectra of the analyte gas phase injection under the same humidity. ES flow rate of 1000 nL min^{-1} for the 2-hexanone solutions and 2000 nL min^{-1} for the L-nicotine solutions. Dependences of the signal area on the concentration are presented in the inserts.

Table 2
Calibration ranges, coefficients of determination, and limits of detection for the linear and non-linear calibrations of the 2-hexanone, fluoroacetamide, L-nicotine, and 1-phenyl-2-thiourea solutions.

	Mode	Linear			Quadratic polynomial		
		Range [mg L^{-1}]	R^2	LOD [mg L^{-1}]	Range [mg L^{-1}]	R^2	LOD [mg L^{-1}]
Short desolvation unit							
2-Hexanone	Pos	0.2–6.5	0.9804	1.5	0.2–32.5	0.9928	2.1
Fluoroacetamide	Pos	0.1–10.0	0.9918	1.5	0.1–40.0	0.9946	2.8
L-Nicotine	Pos	1.0–30.0	0.9576	9.7	1.0–50.0	0.9962	2.3
1-Phenyl-2-thiourea	Pos	0.1–20.0	0.9448	8.3	0.1–40.0	0.9881	4.3
1-Phenyl-2-thiourea	Neg	0.1–20.0	0.9883	3.7	0.1–40.0	0.9980	1.8
Long desolvation unit							
2-Hexanone	Pos	0.5–16.2	0.9954	1.8	0.5–32.5	0.9954	1.9
Fluoroacetamide	Pos	1.0–20.0	0.9897	3.1	1.0–40.0	0.9891	5.3
L-Nicotine	Pos	1.0–30.0	0.9650	8.6	1.0–50.0	0.9929	3.0
1-Phenyl-2-thiourea	Pos	0.1–20.0	0.9874	3.8	0.1–40.0	0.9903	4.1
1-Phenyl-2-thiourea	Neg	0.1–20.0	0.9935	2.8	0.1–40.0	0.9960	2.8

At a constant analyte residence time in the ionization region, the rate of product ion formation can be described by the following equation.

$$r = k[A][\mathrm{RI}] \quad (1)$$

where k is a rate constant of the product ion formation. At very low concentrations the analyte's influence on the reactant ion concentration is negligible ([RI] ≈ const.) and the ionization reaction of the analyte can be described by a pseudo-first order mechanism. In this case, the concentration of the formed product ion should be proportional to the concentration of analyte (linear dependence). At higher analyte concentrations, the concentration of the reactant ion is suppressed and the ionization reaction can be described by a second order mechanism (see Eq. (1), exponential dependence). Under real conditions, the ionization mechanism can be rather complex. Therefore, the relationship between intensity and concentration can differ from the models described here.

Despite the observations described in the previous chapter, the memory effect had a negligible influence on the concentration dependencies, and only minor offsets were observed.

Calibration ranges, coefficients of determination, and limits of detection for the 2-hexanone, fluoroacetamide, L-nicotine, and 1-phenyl-2-thiourea solutions are summarized in Table 2.

The limits of detection for linear regression were calculated as three times the standard deviation of the regression, divided by the slope. In addition to the linear calibration functions, the non-linear second-order calibration functions according to DIN 8466-2 were applied [31]. Use of the non-linear calibration for the ion mobility spectrometry based methods was found to enlarge the range in which the analyte can be quantified. [32] The limits of detection for the linear and non-linear calibration functions are within the same range (1.5–9.7 and 1.8–5.3 g m^{-3} for the linear and non-linear calibration functions, respectively). These limits of detection are rather high for the analytical applications range; hence, further optimizations of the proposed method are required.

The relevant equations for the non-linear calibration can be found in the Supporting information section.

When the pure water was electrosprayed within appropriate flow rates, and the analyte gas phase over the pure compound was mixed with the carrier gas, the results demonstrated a signal appearance at the same compensation voltage for 2-hexanone, fluoroacetamide, and L-nicotine, as in the measurements of the electrosprayed analyte solutions (see Fig. 6). These results support the hypothesis that the droplets entering the ionization region are relatively small, and that the behavior of the electrosprayed analyte in the DMS can be described by the reversible cluster formation model.

In contrast to the results obtained using ES-DMS, no signal was achieved by the mixing of the carrier gas with the gas phase over pure 1-phenyl-2-thiourea, as well as with the gas phase over the saturated 1-phenyl-2-thiourea water solution, at gas phase injection rates of up to 3 mL min^{-1}. This observation demonstrates that even for the compounds of very low volatility (e.g. 1-phenyl-2-thiourea), a sufficient analyte concentration in the carrier gas can be achieved with the current experimental setup. The measurements of analyte solutions of the same concentration demonstrate a signal area within the same range, and with no clear dependence on the compound specific vapor pressure (see Fig. 6 and Supporting information).

4. Conclusion

The feasibility of the ES-^{63}Ni-DMS system for the analysis of liquid samples was proven for water solutions containing four model compounds of different volatility. The usage of an additional ^{63}Ni ionization source, integrated in the DMS chip, led to a high analyte ionization rate and allowed the realization of the coupling, with an arbitrary variable distance between the ES and the detector, with no reduction in the analyte ion concentration prior to the detector region. The electrospray mode and a high stability of the counter gas flow rate were found to be crucial parameters for satisfactory reproducibility. The current desolvation units, installed between the ES source and DMS, have proven to be sufficient for the reduction of the water content in the carrier gas to 2.2–2.4 g m^{-3} and to 1.8–2.0 g m^{-3} for the short and long desolvation units, respectively. The signal position on the CV scale was found to be dependent on humidity; therefore, precise humidity control is important for reliable signal identification. The presence of moisture in the above mentioned concentration range lead to a significant increase in DMS separation ability. With the current experimental setup, which is simple and not optimized, the detection of the model substances in water solutions within a range of 0.1–50 mg L^{-1} was performed, demonstrating the applicability of ES-^{63}Ni-DMS coupling for water samples analysis.

Acknowledgments

This work was financially supported by the Arbeitsgemeinschaft Industrieller Forschungsvereinigungen (AIF), Cologne, (ZIM Project no. KF2210313AK3).

Appendix A. Supplementary material

Supplementary data associated with this article can be found in the online version at http://dx.doi.org/10.1016/j.talanta.2013.10.056.

References

[1] E.V. Krylov, E.G. Nazarov, Int. J. Mass Spectrom. 285 (2009) 149–156. 10.1016/j.ijms.2009.05.009.
[2] I.A. Buryakov, E.V. Krylov, E.G Nazarov, U.Kh. Rasulev, Int. J. Mass Spectrom. Ion Process 128 (1993) 143–148, http://dx.doi.org/10.1016/0168-1176(93)87062-W.
[3] R.A. Miller, E.G. Nazarov, G.A. Eiceman, A.T. King, Sens. Actuators A: Phys. 91 (2001) 301–312, http://dx.doi.org/10.1016/S0924-4247(01)00600-8.
[4] A.A. Shvartsburg, Differential Ion Mobility Spectrometry: Nonlinear Ion Transport and Fundamentals of FAIMS, CRC Press, Boca Raton, 2008.
[5] B.M. Kolakowski, Z. Mester, Analyst 132 (2007) 842–864, http://dx.doi.org/10.1039/b706039d.
[6] S.L. Coy, V.E. Krylov, E.G. Nazarov, A.J. Fornace Jr., R.D. Kidd, Int. J. Ion Mobil. Spectrom. 16 (2013) 217–227, http://dx.doi.org/10.1007/s12127-013-0135-3.
[7] R. Guevremont, J. Chromatogr. A 1058 (2004) 3-19. 10.1016/j.chroma.2004.08.119.
[8] C.M. Whitehouse, R.N. Dreyer, M. Yamashita, J.B. Fenn, Anal. Chem. 57 (1985) 675–679, http://dx.doi.org/10.1021/ac00280a023.
[9] H. Hayen, U. Karst, J. Chromatogr. A 1000 (2003) 549–565, http://dx.doi.org/10.1016/S0021-9673(03)00505-3.
[10] D.B. Robb, T.R. Covey, A.P. Bruins, Anal. Chem. 72 (2000) 3653–3659, http://dx.doi.org/10.1021/ac0001636.
[11] J.A. Syage, M.D. Evans, K.A. Hanold, Am. Lab. 32 (2000) 24–29.
[12] H. Moriwaki, M. Ishitake, S. Yoshikawa, H. Miyakoda, J.F. Alary, Anal. Sci. 20 (2004) 375–377, http://dx.doi.org/10.2116/analsci.20.375.
[13] S.J. Bos, S.M. van Leeuwen, U. Karst, Anal. Bioanal. Chem. 384 (2006) 85–99, http://dx.doi.org/10.1007/s00216-005-0046-1.
[14] E.C. Horning, M.G. Horning, D.I. Carroll, I. Dzidic, R.N. Stillwell, Anal. Chem. 45 (1973) 936–943, http://dx.doi.org/10.1021/ac60328a035.
[15] D.I. Carroll, I. Dzidic, R.N. Stillwell, K.D. Haegele, E.C. Horning, Anal. Chem. 47 (1975) 2369–2373, http://dx.doi.org/10.1021/ac60364a031.
[16] F.W. Karasek, S.H. Kim, S. Rokushika, Anal. Chem. 50 (1978) 2013–2016, http://dx.doi.org/10.1021/ac50036a019.
[17] H. Borsdorf, H. Schelhorn, J. Flachowsky, H.R. Doring, J. Stach, Anal. Chim. Acta 403 (2000) 235–242, http://dx.doi.org/10.1016/S0003-2670(99)00567-X.
[18] A. Jaworek, A.T. Sobczyk, J. Electrost. 66 (2008) 197-219. doi:10.1016/j.elstat.2007.10.001.
[19] Y. Ishihama, H. Katayama, N. Asakawa, Y. Oda, Rapid Commun. Mass Spectrom. 16 (2002) 913–918, http://dx.doi.org/10.1002/rcm.647.
[20] M. Wojdyr, J. Appl. Cryst. 43 (2010) 1126–1128, http://dx.doi.org/10.1107/S0021889810030499.
[21] M. O'neil, A. Smith, P. Heckelman, J. Obenchain, S. Budavari, The Merck Index: Encyclopedia of Chemicals, Drugs and Biologicals, Merck Publications, New Jersey, USA, 1996.
[22] W.B Neely, G.E. Blau, Environmental Exposure From Chemicals, vol. 1, CRC Press, Inc., Boca Raton, FL, 1985.
[23] 2-Hexanone, MSDS No. H2664; J.T. Baker, July 3, 2011.
[24] L-Nicotine, MSDS No. N3876; Sigma, November 21, 2012.
[25] L-Nicotine, MSDS, version 8.8; Merk, June 20, 2013.
[26] N. Krylova, E. Krylov, G.A. Eiceman, J.A. Stone, J. Phys. Chem. A 107 (2003) 3648–3654, http://dx.doi.org/10.1021/jp0221136.
[27] B.B. Schneider, T.R. Covey, S.L. Coy, E.V. Krylov, E.G. Nazarov, Anal. Chem. 82 (2010) 1867–1880, http://dx.doi.org/10.1021/ac902571u.
[28] G.A. Eiceman, Z. Karpas, Ion Mobility Spectrometry, 2nd ed., CRC Press, Boca Raton, 2005.
[29] F. Liang, K. Kerpen, A. Kuklya, U. Telgheder, Int. J. Ion Mobil. Spectrom. 15 (2012) 169–177, http://dx.doi.org/10.1007/s12127-012-0101-5.
[30] G.R. Lambertus, C.S. Fix, S.M. Reidy, R.A. Miller, D. Wheeler, E. Nazarov, R. Sacks, Anal. Chem. 77 (2005) 7563–7571, http://dx.doi.org/10.1021/ac051216s.
[31] Deutsches Institut für Normung e. V (DIN). DIN ISO 8466-2:2001, Berlin, June 2004. Water Quality; Calibration and Evaluation of Analytical Methods and Estimation of Performance Characteristics; Part 2: Calibration Strategy for Non-linear Second-order Calibration Functions.
[32] C. Zscheppank, U. Telgheder, K. Molt, Int. J. Ion Mobil. Spectrom. 15 (2012) 257–264, http://dx.doi.org/10.1007/s12127-012-0097-x.